Local Plastic Response and Slow Heterogeneous Dynamics of Supercooled Liquids

Yan-Wei Li* and Yugui Yao†
Key Laboratory of Advanced Optoelectronic Quantum Architecture and Measurement (MOE), School of Physics,
Beijing Institute of Technology, Beijing, 100081, China

Massimo Pica Ciamarra‡
Division of Physics and Applied Physics, School of Physical and Mathematical Sciences,
Nanyang Technological University, Singapore 637371, Singapore,
CNR–SPIN, Dipartimento di Scienze Fisiche, Università di Napoli Federico II, I-80126, Napoli, Italy
and CNRS@CREATE LTD, 1 Create Way, No. 08-01 CREATE Tower, Singapore 138602, Singapore

(Received 25 January 2022; revised 26 April 2022; accepted 7 June 2022; published 21 June 2022)

We demonstrate, via numerical simulations, that the relaxation dynamics of supercooled liquids correlates well with a plastic length scale measuring a particle's response to impulsive localized perturbations and weakly to measures of local elasticity. We find that the particle averaged plastic length scale vanishes linearly in temperature and controls the super-Arrhenius temperature dependence of the relaxation time. Furthermore, we show that the plastic length scale of individual particles correlates with their typical displacement at the relaxation time. In contrast, the local elastic response only correlates with the dynamics on the vibrational timescale.

DOI: 10.1103/PhysRevLett.128.258001

When supercooled, liquids develop a slow relaxation dynamics [1–3] that proceeds through a sequence of activated events [4]. These relaxation events occur in preferential locations fixed by the particle configuration [5], rather than randomly in space. Furthermore, these events cluster in space and propagate through a facilitation mechanism [6–8], making the dynamics spatially heterogeneous on the relaxation timescale [1–3,9–12]. It is currently unclear what features of a particle configuration identify the regions where relaxation events occur with higher probability.

Previous works suggested that the local structure surrounding each particle determines its possible involvement in irreversible relaxation events and analyzed this structure introducing physically motivated structural parameters [13,13–18] or via machine learning approaches [19,20]. These structural parameters are system dependent as affected, e.g., by the particles' shape. Alternatively, local elastic, rather than geometric, properties may have predictive ability, if the established correlation [21–23] between macroscopic elastic properties and relaxation dynamics also holds at the microscopic scale. Considered measures of local elasticity include the Debye-Waller factor (DWF), its harmonic approximation, and parameters probing particles' vibrational motion [9,24–27]. However, the correlation of a particle's local elastic properties with its involvement in local relaxation processes is debated. Indeed, a particle's vibrational amplitude correlates highly with its short-time displacement [9] but weakly with its displacement evaluated at the relaxation timescale [15]. In addition, correlations between local elastic vibrations and plastic relaxation events entail nonobvious assumptions [28] on the shape of the free energy basin the system is transiently confined.

The response of individual particles to externally applied forces is an alternative approach to characterize local mechanical properties. The response to small forces, which probes the linear elastic regime, revealed the spatial heterogeneity of the local elastic moduli in metallic glasses [29] and dense colloidal suspensions [30]. Larger forces induce plastic flow and allow for microrheology investigations [31–34]. Recently, the response to transient applied forces has been used to probe the emergence of caging in colloidal suspensions [35] and energy absorption in soft colloids [36,37].

In this Letter, we demonstrate that the plastic response induced by transient localized perturbations defines a length ξ that correlates with the relaxation dynamics at the macroscopic and the individual particle level. The average plastic length vanishes linearly with the temperature and regulates the super-Arrhenius divergence of the relaxation time, $\tau = \tau_0 \exp(\xi_0/\xi)$. A particle's local plastic response correlates with its typical displacement at the relaxation time. On the contrary, the local elastic response only correlates with a particle's displacement at shorter times, on the vibrational timescale. Our findings demonstrate that structural relaxation proceeds via local rearrangements that are weakly related to the local elastic response, but well connected to the local plastic response induced by transient perturbations.

We consider the Kob-Andersen [38,39], 65(A):35(B) binary Lennard-Jones mixture of $N = 2000$ particles in two

© 2022 American Physical Society

spatial dimensions. The interaction potential is $U_{\alpha\beta}(r) = 4\epsilon_{\alpha\beta}[(\sigma_{\alpha\beta}/r)^{12} - (\sigma_{\alpha\beta}/r)^{6} + C_{\alpha\beta}]$ for $r \le r^{c}_{\alpha\beta} = 2.5\sigma_{\alpha\beta}$ and $U_{\alpha\beta}(r)=0$ otherwise, $\alpha,\beta \in \{A,B\}$. We set $\sigma_{AB}/\sigma_{AA} = 0.8$, $\sigma_{BB}/\sigma_{AA} = 0.88$, $\epsilon_{AB}/\epsilon_{AA} = 1.5$, $\epsilon_{BB}/\epsilon_{AA} = 0.5$, and fix $C_{\alpha\beta}$ so that the potential vanishes continuously at the cutoff. Length, energy, and time are recorded in units of σ_{AA}, ϵ_{AA}, and $\sqrt{m\sigma^{2}_{AA}/\epsilon_{AA}}$, respectively. We perform Langevin dynamics simulations using LAMMPS [40], numerically integrating the equations of motion, $m\ddot{\mathbf{r}}_i = -\boldsymbol{\nabla}_i \sum_{j(\neq i)} U_{\alpha\beta}(r_{ij}) - \gamma\dot{\mathbf{r}}_i + \eta_i(t)$, where $\mathbf{r}_i$ is the position of the ith particle, r_{ij} is the interparticle distance, and $\gamma = 1$ is the friction coefficient. η_i is a random noise, satisfying $\langle \eta_i(t)\eta_j(t')\rangle = 2k_B T\gamma\delta_{ij}\delta_{t-t'}\mathbf{1}$, with $\mathbf{1}$ the unit tensor. This model has been shown to be a good glass former [39], the relaxation time developing a super-Arrhenius temperature dependence below the onset temperature $T_{\text{onset}} = 0.7$ [41,42], for number density $\rho = 1.2$. We recap the main features of the relaxation dynamics of this model in the Supplemental Material [42].

We probe the local mechanical response by exerting to a particle i of an equilibrium configuration a force of magnitude f and random orientation in the time interval $0 < t < t_p$, mimicking recent experimental studies [30,35–37]. The response of the system depends on f, t_p, and the damping parameter γ. In the following, we concentrate on the f dependence of the response at fixed $\gamma = 1$ and $t_p = 0.1$ corresponding to $\approx 1/10$ of the vibrational timescale. In the Supplemental Material [42], we show that results are robust with respect to changes in γ and t_p as long as the perturbation triggers an irreversible response.

We illustrate in Fig. 1(a) the time dependence of the displacement $\Delta x(t) = \langle \Delta x_i(t_{\text{obs}})\rangle_{\theta,N_r,c}$ induced by a local force of magnitude f. The displacement is averaged over 160 forces differing in their random orientation θ for each particle, and then further averaged over $N_r = 200$ randomly selected particles and $c = 8$ independent configurations. The displacement attains a constant value L for a transient, which approximately ends when the mean-square displacement becomes of order L^2. Below the onset temperature, this transient begins at $t \simeq 2 \times 10^2$, corresponding to roughly $t_{\text{obs}} \simeq 200$ vibrational times.

The time dependence of the displacement informs on the elastic properties of the systems. Indeed, in a viscous medium, the displacement induced by a transient localized force increases monotonically and saturates to a plateau value, $L \propto f$. In Fig. 1(a), where dashed lines mark the value of L, we observe this behavior at the largest of the considered temperatures. In contrast, in a viscoplastic medium, the displacement reaches a maximum and then saturates to a smaller L value, as we observe at the other considered temperatures. In the presence of a purely elastic response, the final displacement L would vanish.

The magnitude of the average force-induced displacement $L(T,f)$ (see Fig. S4 in the Supplemental Material [42] for the distribution of the individual particle displacements) depends on the applied force and temperature. Below the onset temperature, the asymptotic displacement increases linearly with the temperature $L(T,f) \propto (T - T_0)$ and with the applied force $L \propto (f - f_0)$, as illustrated in Figs. 1(b) and 1(c). Here, $T_0 \simeq 0.12$ and f_0 is a temperature-independent threshold value. This scaling does not hold at

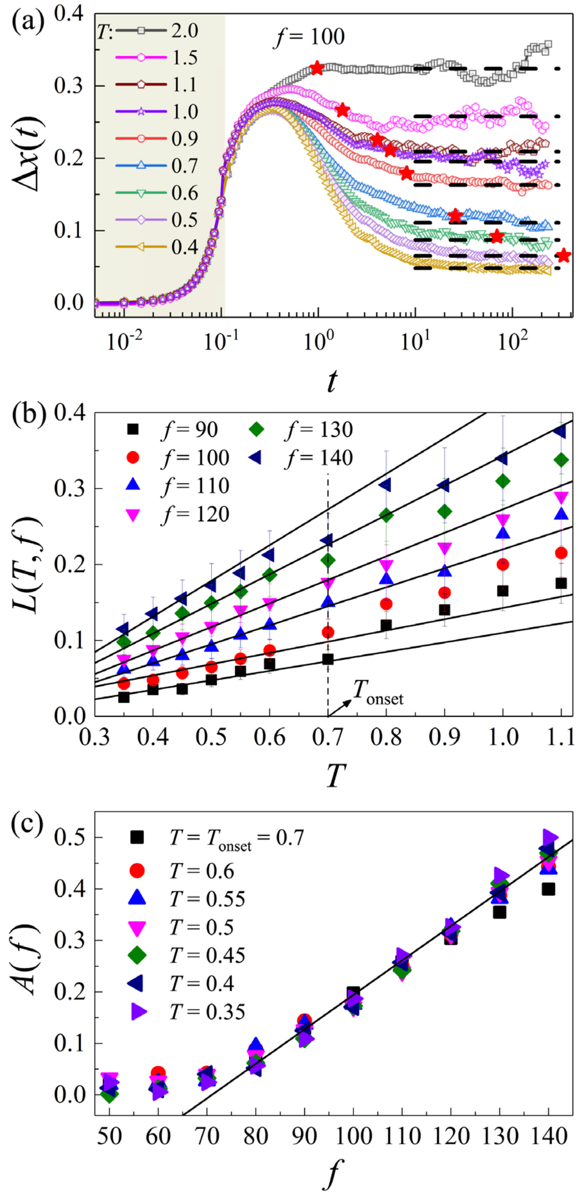

FIG. 1. (a) Time dependence of the average displacement of a particle in response to a force acting on the time window identified by the shaded region. The dashed lines mark the asymptotic displacement values $L(T,f)$. The filled red stars mark the $\Delta x(\tau_{\text{CR}})$ for $T \ge 0.5$. (b) The asymptotic displacement grows linearly in temperature below the onset temperature marked by the vertical dashed line, $L \propto (T - T_0)$. (c) A plot of $A(f) = L(T,f)/(T - T_0)$ reveals that, below the onset temperature, the asymptotic displacement grows linearly in f for large enough forces.

higher temperatures (see Fig. S3 [42]), and indeed, a small deviation already occurs at the onset temperature in Fig. 1(c). The need of applying a minimum force to induce irreversible particle motion is consistent with previous results [34].

To rationalize the force dependence of L, we investigate the response to the application of localized forces of systems brought in energy minima in the Supplemental Material [42]. This investigation suggests that the temperature independence of f_0 reflects the weak dependence of the energy landscape on the temperature of the parent liquid, in the supercooled regime, and that L has a linear dependence on f as it results from the accumulation of $n(f) \propto (f - f_0)$ plastic displacements of typical size $\langle l \rangle$ [42].

Summarizing, Fig. 1 shows that, in the regime of low temperature and forces large enough to trigger plastic rearrangements, the force-induced displacement varies as $L(T,f) = \xi(T)(1 - f/f_0)$, with $\xi(T) \propto (T - T_0)$ a temperature-dependent length scale. Next, we show that this plastic length regulates the relaxation dynamics.

We probe the relaxation dynamics using cage-relative (CR) measures to filter out the influence of long-wavelength fluctuations [41,43–46] that lead to an underestimation of the structural relaxation time in two spatial dimensions. While standard relaxation measures focus on the actual displacement of each particle, CR measures focus on the displacement of a particle with respect to the average displacement of its neighbors, which we identify via the Voronoi construction. This definition makes CR measures unaffected by the collective translations that characterize long-wavelength fluctuations.

We estimate the CR relaxation time $\tau_{\rm CR}(T)$, which is proportional to the shear viscosity [41,47], from the decay of the CR self-scattering function evaluated at the wave vector corresponding to the first peak of the structure factor. Figure 2 illustrates that, below the onset temperature, the CR relaxation time grows exponentially with the inverse plastic length scale $\xi(T)$,

$$\tau_{\rm CR}(T) = \tau_0 \exp\left(\frac{\xi_0}{\xi(T)}\right), \tag{1}$$

with τ_0 a microscopic vibrational timescale and ξ_0 a constant. Given that $\xi \propto (T - T_0)$, Eq. (1) corresponds to a Vogel-Fulcher-Tammann (VFT) dependence of the relaxation time on temperature, which we illustrate in Fig. S2 of the Supplemental Material [42].

We stress that other functional forms may describe the super-Arrhenius temperature dependence of the relaxation time. As such, we do not want to give fundamental significance to the fitting parameters. Yet, since $\tau = \tau_0 \exp(\Delta F/T)$, where $\Delta F(T)$ is the free energy barrier of the elementary relaxation events, our finding demonstrates a connection between the plastic length scale $\xi(T)$ and $\Delta F(T)$, i.e., $\Delta F \propto 1/\xi$. This is our first main result.

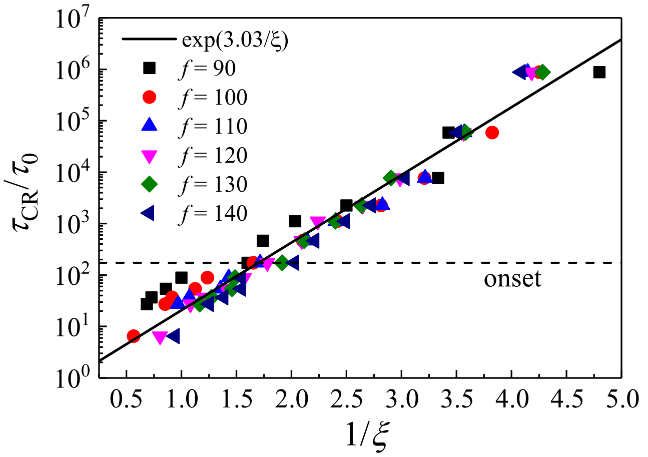

FIG. 2. The cage-relative relaxation time grows exponentially with the reciprocal plastic length $1/\xi(T) = (1-f/f_0)(1-T/T_0)/L(T,f)$. Data refer to $\rho = 1.2$.

A VFT-like divergence of the relaxation time is predicted by entropic theories of the glass transition, such as the early Adam-Gibbs [48] scenario and the subsequent random first-order transition theory [49]. According to these theories, the super-Arrhenius dynamics follows from the vanishing of the configurational entropy or, equivalently, from the divergence of a static length that measures the size of loosely defined cooperative rearranging regions [50,51]. Previous works supported the existence of a growing static length on cooling [11,13,18,52–55]. These theories are consistent with our results only if the dynamical slowdown involves both a decreasing and an increasing length scale. This scenario may occur if relaxation events have a core-corona structure, with the core and corona size respectively decreasing and increasing on cooling. In this respect, we remark that particles undergoing large displacements in a relaxation event become increasingly localized [56,57] on cooling.

Elastic models of the glass transitions [21,58] relate ΔF to a vanishing length scale, the DWF, e.g., $\Delta F \propto 1/\langle u^2 \rangle^{\alpha/2}$ with α a phenomenological parameter describing cage anisotropy [23,59] or related functional forms [22,24]. While both ξ and $\langle u^2 \rangle$ decrease on cooling, these lengths are conceptually different. ξ relates to the plastic response and it appears to vanish at a finite temperature. In contrast, $\langle u^2 \rangle$ probes the elastic, possibly anharmonic, vibrational motion and only vanishes at zero temperature. Indeed, to recover a super-Arrhenius behavior, earlier works [24] suggested the relaxation time relates to the difference between $\langle u^2 \rangle$ and its expected crystalline value.

We now turn our attention to the spatial and temporal heterogeneity of the relaxation dynamics [1–3], which we quantify by resorting to the CR mean-square displacement in the isoconfigurational ensemble [5]. We evaluate $\langle \Delta r^2_{i,\rm CR}(t) \rangle_{\rm iso}$ by averaging the mean-square displacement of each particle over 128 equilibrium simulations sharing the same initial particle configuration and differing in the particles' momenta, we randomly sample from the relevant equilibrium distribution. Particles with a large $\langle\Delta r^2_{i,\mathrm{CR}}(t)\rangle_{\mathrm{iso}}$ at the relaxation time identify the locations more prone to structural rearrangements [5,9].

We investigate the correlations between $\langle\Delta r^2_{i,\mathrm{CR}}(t)\rangle_{\mathrm{iso}}$ and a local plastic length scale $\xi_i = \langle\Delta x_i(t_{\mathrm{obs}})\rangle_\theta$, which we define as the displacement induced by the application of a randomly oriented force of magnitude $f = 140$ on particle i, averaged over 200 realizations. To compare with previous works [6,9,15], we also investigate how $\langle\Delta r^2_{i,\mathrm{CR}}(t)\rangle_{\mathrm{iso}}$ correlates with the CR-DWF $\langle u_i^2\rangle = \langle\Delta r^2_{i,\mathrm{CR}}(\tau_\beta)\rangle_{\mathrm{iso}}$, the mode participation p_i [9], and the harmonic mean-square displacement ψ_i [15]. Here τ_β is the time at which the logarithmic derivative of the mean-square displacement acquires its minimum, implying that the system is maximally subdiffusive [22]. To evaluate p and ψ, we diagonalize the Hessian matrix of the disordered solid obtained by minimizing the energy of the $t = 0$ configuration via the TINKER package [60], obtaining $2N - 2$ eigenmodes $\mathbf{e}(\omega_a)$ with nonzero eigenfrequencies ω_a. We define the participation fraction of particle i as $p_i = \langle|\mathbf{e}_i(\omega_j)|^2\rangle_{N_m}$, where j runs over the $N_m = 50$ modes with lowest nonzero frequency. The mean-square displacement in the harmonic approximation is $\psi_i = \sum_a \omega_a^{-2}|\mathbf{e}_i(\omega_a)|^2$. At each time t, we resort to Spearman's rank correlation coefficient $S(t)$ [11,61–63] to evaluate how $\langle\Delta r^2_{\mathrm{CR}}(t)\rangle_{\mathrm{iso}}$ correlates to each of the different considered static quantities. $S = 1$ (-1) for monotonically increasing (decreasing) dependence of two quantities, while $S = 0$ in the absence of correlations.

Figure 3 illustrates (right axis) the time evolution of the average CR mean-square displacement at $\rho = 1.2$ and $T = 0.4$, and (left axis) the time evolution of Spearman's rank correlation coefficients. By definition, $\langle\Delta r^2_{i,\mathrm{CR}}(t)\rangle_{\mathrm{iso}}$ and $\langle u_i^2\rangle$ are perfectly correlated at $t{=}\tau_\beta$ ($\tau_\beta \simeq 3\times 10^{-4}\tau_{\mathrm{CR}}$ at $\rho = 1.2$ and $T = 0.4$). Figure 3 clarifies that the correlation sharply drops at longer times [15], equaling $\simeq 0.1$ at the relaxation timescale. Similarly, the correlation between $\langle\Delta r^2_{i,\mathrm{CR}}(t)\rangle_{\mathrm{iso}}$ and both participation fraction and mean-square displacement in the harmonic approximation reaches a maximum at short times and sensibly drops on the relaxation timescale.

These results agree with previous investigations [9] on the relation between isoconfigurational mean-square displacement and participation fraction, that found correlations at $t \simeq 0.3\tau$, with τ the relaxation time evaluated without resorting to CR measures [64]. Indeed, for the system considered in Fig. 3, $t = 0.3\tau$ corresponds to $t \simeq 0.1\tau_{\mathrm{CR}}$, a short time where the dynamics is still dominated by the vibrational motion. The critical conclusion we reach from this investigation is that participation fraction and DWF correlate well with the vibrational dynamics but weakly with the dynamics on the relaxation timescale. Henceforth, these quantities are not a good proxy for the location of the relaxation events.

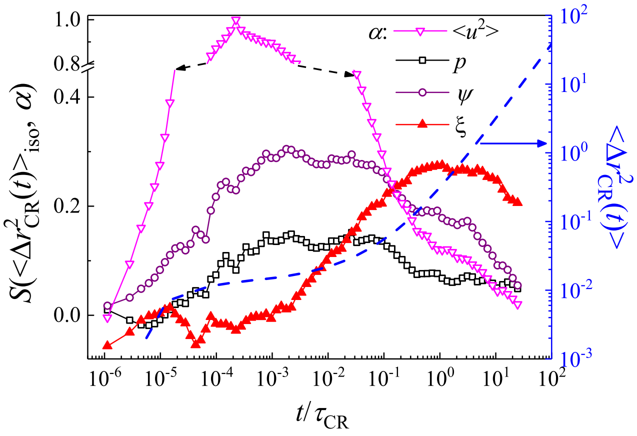

FIG. 3. Time dependence of Spearman's rank correlation coefficient S between the CR mean-square displacement of the particles at time t and (1) their CR mean-square displacement at $t = \tau_\beta$, (2) their participation fraction p, (3) their mean-square displacement evaluated in the harmonic approximation, and (4) their plastic length scale ξ. The blue dashed line represents the average CR mean-square displacement.

In Fig. 3, we also illustrate Spearman's rank correlation coefficient between $\langle\Delta r^2_{i,\mathrm{CR}}(t)\rangle_{\mathrm{iso}}$ and the plastic length scale ξ_i. This correlation coefficient is small at short times and reaches a maximum at the relaxation time. Hence, it critically differs from the other correlation coefficients we have investigated that peak on the vibrational timescale. These findings demonstrate that the plastic length scale is a robust indicator of the relaxation dynamics at the particle level. This result is our second significant result.

To further test the validity of our results, we have replaced $\langle\Delta r^2_{i,\mathrm{CR}}(t)\rangle_{\mathrm{iso}}$ with alternative measures of structural relaxation, a particle-based self-scattering function and the fraction of neighbors the particle has lost at time t. Figure S11 in [42] shows that our findings are robust with respect to the adopted definition of local structural relaxation. In addition, in the Supplemental Material we show that the average plastic length scale correlates with the relaxation time, and the locally defined plastic length scale identifies the particles more prone to rearrange, also when the dynamical slowdown is induced by an increase of the density at a constant temperature. These investigations support the robustness of our findings and clarify that our predictions could be experimentally tested in suspensions of colloidal particles [30,35–37], where density is the main control parameter.

Our results show that the response of individual particles to transient, almost impulsive perturbations defines a plastic correlation length that regulates supercooled liquids' relaxation dynamics. The average plastic correlation length ξ is inversely proportional to the free energy barrier $\Delta F(T)$ governing the dynamic slowdown. The plastic response of individual particles informs on their participation in localized relaxation events and hence on the spatial heterogeneity of the relaxation process at the relaxation timescale. Our findings provide novel insights into the origin of slow and heterogeneous dynamics, showing that the local elastic response mostly correlates with the vibrational dynamics rather than with the dynamics at the relaxation time. Our results may inspire novel glass transition theories and stimulate experimental research on the plastic response to external forces induced, e.g., by laser pulses.

We thank M. Wyart for fruitful discussions. Y.-W. L. acknowledges support of the start-up funding of Beijing Institute of Technology and support from the National Natural Science Foundation (NSF) of China (Grant No. 12105012). Y. Y. is supported by the NSF of China (Grants No. 11734003 and No. 12061131002). M. P. C. acknowledges support from the Singapore Ministry of Education through the Singapore Academic Research Fund (MOE2019-T1-001-03 and MOE2019-T1-001-22) and the National Supercomputing Centre Singapore (NSCC) for the computational resources.

---

[*] yanweili@bit.edu.cn
[†] ygyao@bit.edu.cn
[‡] massimo@ntu.edu.sg

[1] M. D. Ediger, Annu. Rev. Phys. Chem. **51**, 99 (2000).
[2] P. Debenedetti and F. Stillinger, Nature (London) **410**, 259 (2001).
[3] L. Berthier and G. Biroli, Rev. Mod. Phys. **83**, 587 (2011).
[4] M. Pica Ciamarra, R. Pastore, and A. Coniglio, Soft Matter **12**, 358 (2016).
[5] A. Widmer-Cooper, P. Harrowell, and H. Fynewever, Phys. Rev. Lett. **93**, 135701 (2004).
[6] R. Candelier, A. Widmer-Cooper, J. K. Kummerfeld, O. Dauchot, G. Biroli, P. Harrowell, and D. R. Reichman, Phys. Rev. Lett. **105**, 135702 (2010).
[7] A. S. Keys, L. O. Hedges, J. P. Garrahan, S. C. Glotzer, and D. Chandler, Phys. Rev. X **1**, 021013 (2011).
[8] R. Pastore, A. Coniglio, and M. Pica Ciamarra, Soft Matter **11**, 7214 (2015).
[9] A. Widmer-Cooper, H. Perry, P. Harrowell, and D. Reichman, Nat. Phys. **4**, 711 (2008).
[10] A. S. Keys, L. O. Hedges, J. P. Garrahan, S. C. Glotzer, and D. Chandler, Phys. Rev. X **1**, 021013 (2011).
[11] H. Tong and H. Tanaka, Phys. Rev. X **8**, 011041 (2018).
[12] Y.-C. Hu, Y.-W. Li, Y. Yang, P.-F. Guan, H.-Y. Bai, and W.-H. Wang, Proc. Natl. Acad. Sci. U.S.A. **115**, 6375 (2018).
[13] T. Kawasaki, T. Araki, and H. Tanaka, Phys. Rev. Lett. **99**, 215701 (2007).
[14] C. Patrick Royall, S. R. Williams, T. Ohtsuka, and H. Tanaka, Nat. Mater. **7**, 556 (2008).
[15] R. L. Jack, A. J. Dunleavy, and C. P. Royall, Phys. Rev. Lett. **113**, 095703 (2014).
[16] A. Furukawa, Phys. Rev. E **97**, 022615 (2018).
[17] Y.-W. Li, Y.-L. Zhu, and Z.-Y. Sun, Phys. Rev. E **94**, 062601 (2016).
[18] K. Watanabe, T. Kawasaki, and H. Tanaka, Nat. Mater. **10**, 512 (2011).
[19] E. D. Cubuk, S. S. Schoenholz, J. M. Rieser, B. D. Malone, J. Rottler, D. J. Durian, E. Kaxiras, and A. J. Liu, Phys. Rev. Lett. **114**, 108001 (2015).
[20] S. S. Schoenholz, E. D. Cubuk, D. M. Sussman, E. Kaxiras, and A. J. Liu, Nat. Phys. **12**, 469 (2016).
[21] J. C. Dyre, Rev. Mod. Phys. **78**, 953 (2006).
[22] L. Larini, A. Ottochian, C. De Michele, and D. Leporini, Nat. Phys. **4**, 42 (2008).
[23] B. A. Pazmiño Betancourt, P. Z. Hanakata, F. W. Starr, and J. F. Douglas, Proc. Natl. Acad. Sci. U.S.A. **112**, 2966 (2015).
[24] U. Buchenau and R. Zorn, Europhys. Lett. **18**, 523 (1992).
[25] A. Smessaert and J. Rottler, Soft Matter **10**, 8533 (2014).
[26] M. Mosayebi, P. Ilg, A. Widmer-Cooper, and E. Del Gado, Phys. Rev. Lett. **112**, 105503 (2014).
[27] A. Widmer-Cooper and P. Harrowell, Phys. Rev. Lett. **96**, 185701 (2006).
[28] A. Kumar, I. Procaccia, and M. Singh, Europhys. Lett. **135**, 66001 (2021).
[29] H. Wagner, D. Bedorf, S. Kchemann, M. Schwabe, B. Zhang, W. Arnold, and K. Samwer, Nat. Mater. **10**, 439 (2011).
[30] D. Anderson, D. Schaar, H. G. E. Hentschel, J. Hay, P. Habdas, and E. R. Weeks, J. Chem. Phys. **138**, 12A520 (2013).
[31] P. Habdas, D. Schaar, A. C. Levitt, and E. R. Weeks, Europhys. Lett. **67**, 477 (2004).
[32] A. M. Puertas and T. Voigtmann, J. Phys. Condens. Matter **26**, 243101 (2014).
[33] E. M. Furst and T. M. Squires, *Microrheology* (Oxford University Press, Oxford, 2018), Vol. 1.
[34] N. Şenbil, M. Gruber, C. Zhang, M. Fuchs, and F. Scheffold, Phys. Rev. Lett. **122**, 108002 (2019).
[35] B. Li, K. Lou, W. Kob, and S. Granick, Nature (London) **587**, 225 (2020).
[36] J. M. van Doorn, R. Higler, R. Wegh, R. Fokkink, A. Zaccone, J. Sprakel, and J. van der Gucht, Sci. Adv. **6**, eaba6601 (2020).
[37] I. Buttinoni, J. Cha, W.-H. Lin, S. Job, C. Daraio, and L. Isa, Proc. Natl. Acad. Sci. U.S.A. **114**, 12150 (2017).
[38] W. Kob and H. C. Andersen, Phys. Rev. Lett. **73**, 1376 (1994).
[39] R. Brüning, D. A. St-Onge, S. Patterson, and W. Kob, J. Phys. Condens. Matter **21**, 035117 (2009).
[40] S. Plimpton, J. Comput. Phys. **117**, 1 (1995).
[41] Y.-W. Li, C. K. Mishra, Z.-Y. Sun, K. Zhao, T. G. Mason, R. Ganapathy, and M. Pica Ciamarra, Proc. Natl. Acad. Sci. U.S.A. **116**, 22977 (2019).
[42] See Supplemental Material at http://link.aps.org/supplemental/10.1103/PhysRevLett.128.258001 for additional information on the slow dynamics, plastic length distribution, role of damping parameter, force duration and force magnitude, plastic length at $T = 0$, alternative measure of structural relaxation, and density dependence of the plastic length.

[43] N. D. Mermin and H. Wagner, Phys. Rev. Lett. **17**, 1133 (1966).

[44] H. Shiba, Y. Yamada, T. Kawasaki, and K. Kim, Phys. Rev. Lett. **117**, 245701 (2016).

[45] S. Vivek, C. P. Kelleher, P. M. Chaikin, and E. R. Weeks, Proc. Natl. Acad. Sci. U.S.A. **114**, 1850 (2017).

[46] B. Illing, S. Fritschi, H. Kaiser, C. L. Klix, G. Maret, and P. Keim, Proc. Natl. Acad. Sci. U.S.A. **114**, 1856 (2017).

[47] H. Shiba, T. Kawasaki, and K. Kim, Phys. Rev. Lett. **123**, 265501 (2019).

[48] G. Adam and J. H. Gibbs, J. Chem. Phys. **43**, 139 (1965).

[49] T. R. Kirkpatrick, D. Thirumalai, and P. G. Wolynes, Phys. Rev. A **40**, 1045 (1989).

[50] J. D. Stevenson, J. Schmalian, and P. G. Wolynes, Nat. Phys. **2**, 268 (2006).

[51] C. Donati, J. F. Douglas, W. Kob, S. J. Plimpton, P. H. Poole, and S. C. Glotzer, Phys. Rev. Lett. **80**, 2338 (1998).

[52] G. Biroli, J.-P. Bouchaud, A. Cavagna, T. S. Grigera, and P. Verrocchio, Nat. Phys. **4**, 771 (2008).

[53] S. Karmakar, C. Dasgupta, and S. Sastry, Annu. Rev. Condens. Matter Phys. **5**, 255 (2014).

[54] K. Hima Nagamanasa, S. Gokhale, A. K. Sood, and R. Ganapathy, Nat. Phys. **11**, 403 (2015).

[55] Z. Zheng, R. Ni, Y. Wang, and Y. Han, Sci. Adv. **7**, eabd1958 (2021).

[56] D. Coslovich, A. Ninarello, and L. Berthier, SciPost Phys. **7**, 077 (2019).

[57] W. Ji, T. W. J. de Geus, M. Popović, E. Agoritsas, and M. Wyart, Phys. Rev. E **102**, 062110 (2020).

[58] R. W. Hall and P. G. Wolynes, J. Chem. Phys. **86**, 2943 (1987).

[59] D. S. Simmons, M. T. Cicerone, Q. Zhong, M. Tyagi, and J. F. Douglas, Soft Matter **8**, 11455 (2012).

[60] J. W. Ponder and F. M. Richards, J. Comput. Chem. **8**, 1016 (1987).

[61] C. Sammut and G. I. Webb, *Encyclopedia of Machine Learning* (Springer-Verlag, Berlin, 2011).

[62] A. Widmer-Cooper and P. Harrowell, J. Non-Cryst. Solids **352**, 5098 (2006).

[63] G. M. Hocky, D. Coslovich, A. Ikeda, and D. R. Reichman, Phys. Rev. Lett. **113**, 157801 (2014).

[64] D. N. Perera and P. Harrowell, J. Chem. Phys. **111**, 5441 (1999).